

UVP Measurement of a Turbulent Channel Flow Containing Large Bubbles

Yuichi Murai, Hideki Fujii, Yuji Tasaka and Yasushi Takeda

Div. Energy & Env. System, School of Engineering, Hokkaido University, 060-8628, Sapporo, Japan

UVP has been applied to measurement of gas-liquid two-phase flow in a horizontal channel. The original data acquired by UVP is transformed by a filter that extracts interfaces of bubbles. The best filter is chosen among several candidates to accurately obtain liquid volume flow rate. Conditional averaging for liquid phase provides valid mean velocity profiles that have been altered significantly by presence of bubbles. The modified flow field by the bubbles involves accelerated region of liquid owing to reduction of skin friction through the bubbles. Whilst local turbulent intensity increases there monotonically with increment of both flow rates, it takes the highest value at the near-wall void fraction of around 2%.

Keywords: Multiphase Flow, turbulent flow, drag reduction, bubble dynamics, UVP, interfacial detection, air-film method, channel flow

1 INTRODUCTION

Ultrasound velocity profiler (UVP) is applied to measurements of water flow structure in a turbulent channel flow in which cm-order bubbles are mixed. The purpose of this study is originally planned to investigate the mechanism of frictional drag reduction provided by air bubbles. For the same purpose a number of experimental approaches were reported to date, such as by Hotwire, LDV [1], optical probe and PIV [2-3]. In our lab., UVP or ultrasound Doppler-base technique has been newly introduced to the elucidation of the flow structure altered through bubbles. Extension of UVP measurements to bubbly two-phase flow was first reported by Suzuki et al[4]. Their method was based on detection of the local maximum velocity in each instant profile to identify the bubble interface in a counter-current vertical two-phase flow. Eckert et al[5] developed an ultrasound transducer applicable for high temperature liquid metal containing rising bubbles in a bath. They detected velocity of bubbles smaller than the effective beam diameter, referring spatio-temporal diagram of liquid velocity profiles. Murakawa et al[6] reported the use of two ultrasound transducers with different frequencies for capturing the motion of size-dependent bubbles' in a pipe flow. An excellent application of UVP to a pipe flow containing a large buoyant bubble was recently reported by Minagawa et al[7] who obtained average velocity profiles using two ultrasound transducers to measure the average velocity vector field. This paper deals with a method for signal processing of UVP-output to detect the gas-liquid interface without using optical information. This work is positioned as an intermediate but indispensable step on a way to achieve an ultrasound sensing of drag reduction phenomena. Our future application is of a complete monitoring of bubbly two-phase boundary layer only using UVP but not introducing any other tool for the interface detection since this

technique is desired to be applied to ships and pipelines.

2 MEASUREMENT METHOD

2.1 Target of Flow Measurement

Fully developed turbulent two-phase flow in a horizontal rectangular channel is measured. The schematic is shown in Fig.1. The size of the channel is 40mm in height, 160mm in lateral width, and 6m in length. Tap water and room air are used as two phases. Bubbles are injected through several capillary tubes mounted on the upper surface of the channel. Size of the bubbles ranges from 10mm to 100mm, which is larger than the effective beam diameter of ultrasound. Mean flow velocity varies within $0.3 < U < 1.5$ m/s, corresponding to Re number of 1.2 to 6.0×10^4 . Measurement position of UVP is located at 920mm ($x/H=23$) downstream of the bubble injection point. Tracer particles, with density and mean diameter of 1020 kg/m³ and 200 μ m, are seeded in the water as an ultrasound reflector. We tested the quality of velocity-acquisition, which depends on the number density of the particles and concluded that 10^7 per m³ was sufficient.

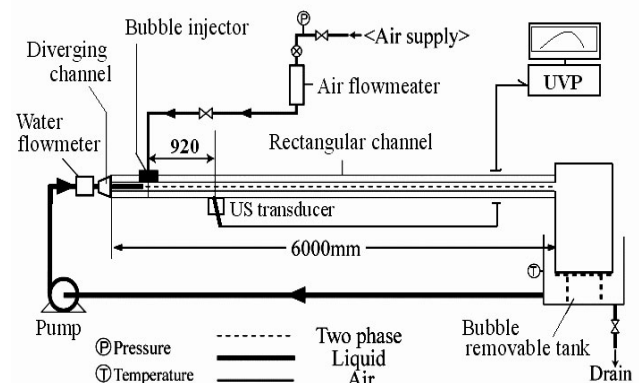


Figure 1: Experimental facility

2.2 UVP Specification

Head of an ultrasound transducer is fixed below the bottom channel wall with inclination angle of 5.0 degree. Measurement lines thus is oriented nearly upward to capture the velocity profile as function of the vertical coordinate while bubbles are mainly suspended near the upper wall. The head diameter of the transducer is 5mm. A commercial processor (MetFlow SA, UVP-DUO) is used to control the ultrasound wave and to process the echo signal for acquiring the velocity profile. The transducer emits a pulsed ultrasound with basic frequency of 4MHz and pulse-repetition frequency of 6.6kHz. The sampling rate is 30Hz, which means that the velocity data are output as ensemble averaging of pulse-by-pulse velocity information during 1/30 s, as around 128 shots of pulse.

2.3 Spatial Resolution Relative to Bubble Size

Fig.2 shows several samples of bubble images taken from the top of the channel at $Re=2.8 \times 10^4$. The picture size is 160mmx160mm. Symbol α denotes the bulk average void fraction defined by volume flow rates of two phases: $\alpha = Q_G / (Q_L + Q_G)$. The bubbles migrate from left to right in the picture. The maximum Weber number; $We = \rho U^2 d / \sigma$ (ρ : density of liquid, d : bubble diameter, σ : surface tension) is 10^3 and hence individual bubbles are considerably deformed with the inertia of liquid flow. The thickness of the lateral double lines in the figure stands for the effective beam thickness of UVP, which is estimated at around 7mm, being smaller than the bubble size.

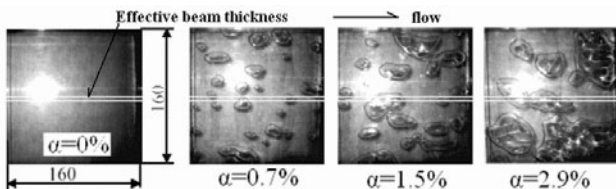


Figure 2: Beam streak and bubbles

2.4 Ultrasound Behavior about Interface

Ultrasound mostly reflects on the gas-liquid interface due to the large difference in acoustic impedance. The ultrasound phase is reversed during reflection because of the fixed pressure (here, a small closed interface such as microbubble is an exception because of the strong surface tension). Thus, local standing waves occur within a length of pulsed ultrasound from the interface. Fig.3 shows the wave behavior of pulsed ultrasound as it reflects on the interface, analyzed by a one-dimensional wave equation. The lateral coordinate is time evolution. In the case of a four-cycle pulse that is used in the present UVP, four layers of weak pressure regions come out due to the local standing waves. The particles existing inside these layers do not produce

significant echo that no longer involve regular Doppler information. The internal program of a commercial UVP processor outputs zero-velocity in such a region. The particles existing on peak region of the standing wave has two echoes produced by advancing and returning waves so that the composed wave has no Doppler shift frequency though the individual shift exists. Consequently UVP outputs nearly zero velocity inside the standing wave region regardless the real velocity. Therefore the interface can be detected by finding such a layer out of the data. The thickness of the standing wave in the normal direction to the interface is estimated by

$$\delta = \frac{1}{2} \lambda k \cos \theta \tag{1}$$

where λ , k , and θ are the wavelength of the ultrasound, the cycle number of single pulse, and the inclination angle of the measurement line. The estimated thickness is about 0.74mm in the case of 4-cycle-pulsed 4MHz-ultrasound.

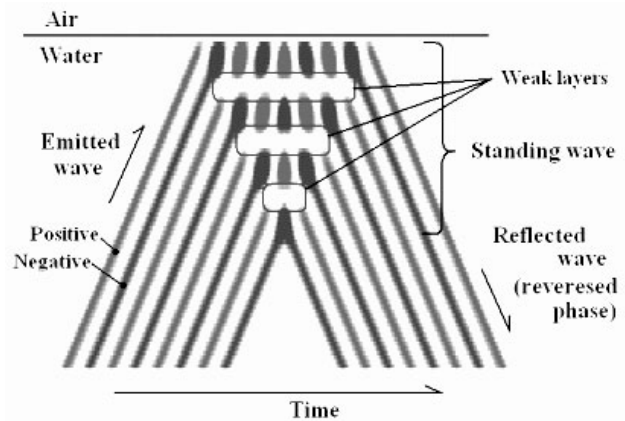


Figure 3: Reflection of pulsed ultrasound on interface

2.5 Interface Detection Algorithm

Fig.4 shows a sample of the procedure to detect bubble interfaces. Brightness of each map is a) original velocity measured by UVP, b) a filtered image, and c) resultant interfaces obtained. The filter employed eventually is Sobel filter, which smoothens temporal noise and takes vertical gradient in space simultaneously. The filter well captures the bottom interface of individual bubbles. We examined other types of filters including Laplacian filter, high-pass and band-pass filters to conclude that Sobel filter works the best. The resultant interface is verified by the flow rates measured by flow meters. For instance, the liquid flow rate estimated by integrating the mean velocity profile inside liquid phase matches the flow rate directly measured by a floating type flow meter within 5% error. Note that the applicability of the present method is limited to the case that bubbles have nearly flat bottom interface longer than the beam diameter. The method needs to be improved

when the flow contains small bubbles or high turbulent bubbles.

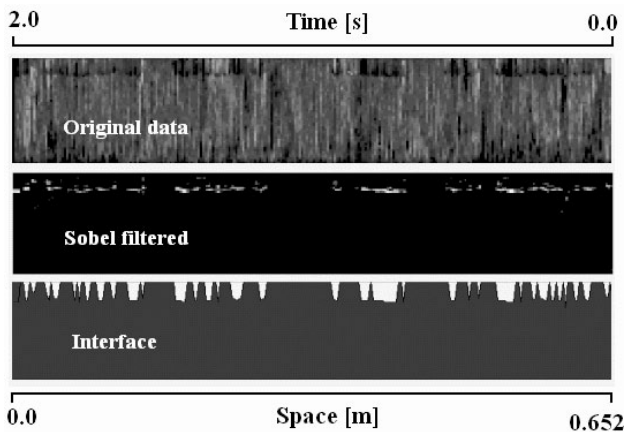


Figure 4: Bubble interfaces detected by Sobel filter

3 MEASUREMENT RESULTS

3.1 Mean Profiles of Bubbly Channel

Fig.5 shows comparison of mean profiles, where u : mean liquid velocity, α : mean void fraction, and q : turbulent intensity. The mean liquid velocity is calculated by conditional averaging of velocity inside the liquid, using the interface information. The void fraction is calculated by the ratio of liquid phase to the total sampling period. The bulk void fraction can be calculated by averaging all the profile in the vertical direction and it matched the one given by the two flow meters within 5%. Local void fraction just on the upper wall corresponds to the bubble-covering ratio, to which drag reduction generally works proportionally. The turbulent intensity q is here defined by the on-beam component fluctuation of velocity. Therefore q distributes asymmetrically even in the symmetrical single-phase channel flow because of inclined measurement line[8]. The data show that the liquid velocity increases inside the bubbly layer. This is caused by advection effect of bubbles that have finite deformation. The turbulent intensity increases in the border region between the bubbly layer and the outer region, or the high gradient-region of void fraction.

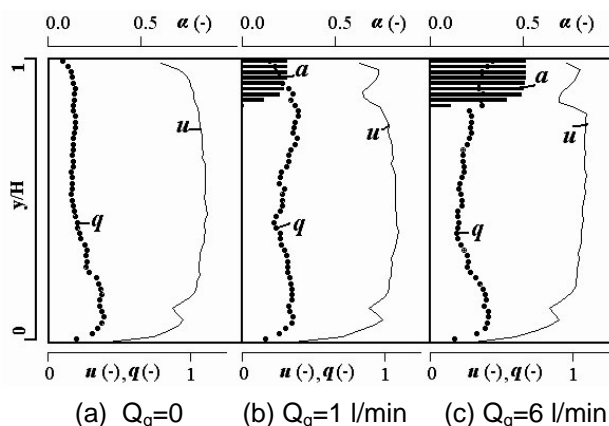


Figure 5: Mean profiles of bubbly channel at $Re=1.2 \times 10^4$

3.2 Velocity Field Modified by Bubbles

To clearly see the effect of bubbles on the liquid flow structure, the modified component of velocity is extracted by subtracting the mean velocity profile of single-phase turbulent flow. Fig.6 shows those in four different bulk void fractions. White region indicates high-speed parts relative to the mean value. In the single-phase flow ($\alpha=0$), the high-speed parts emerge semi-periodically near the two walls. Such events correspond to momentum mixing in turbulent shear flows, and those distribute symmetrically in the vertical direction. After bubbles are injected, accelerated parts come out in the vicinity of the upper wall. This is caused by the interaction between the bubbles and the boundary layer, that is, the bubbles are driven in the flow direction by the liquid but simultaneously resist against the deformation owing to the surface tension. With this force balance, the bubbles that migrate with keeping their shape provide accelerated layer in the vicinity of the wall. This acceleration promotes the increment of local skin friction while the total skin friction tends to decrease with the bubble-occupying area on the wall. Another finding is also confirmed in the figures, which is propagation of high-speed region from the top to the bottom part. The propagation begins on the rear edge of individual bubbles and advances downward with around 45 degree in space. This implies that the drag reduction effect provided by individual single bubbles alters the flow within a certain spatial/temporal scale.

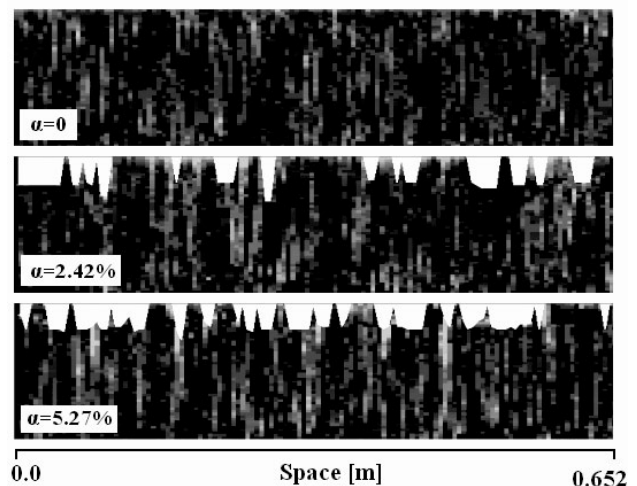


Figure 6: Modified component of velocity at $Re=1.2 \times 10^4$

3.3 Turbulent Intensity inside Bubbly Layer

Fig.7 shows the turbulent intensity q , which is averaged inside the bubbly layer. The sampling height of the bubbly layer is fixed at $0.16H$ according to the void fraction profile. The graph tells us that the turbulence increases with mean velocity (or Re number) almost monotonically, and also that the mixing of bubbles enhances the turbulence. This

trend is generally inverse to the microbubble drag reduction. Microbubble drag reduction utilizes the suppression of the turbulence inside the boundary layer. The use of bubbles much larger than the turbulent eddy scale makes the turbulence event stronger.

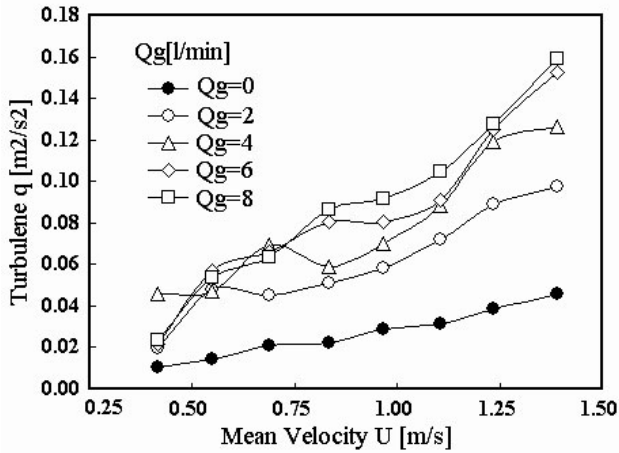


Figure 7: Turbulent intensity inside bubbly layer; $y/H < 0.16$

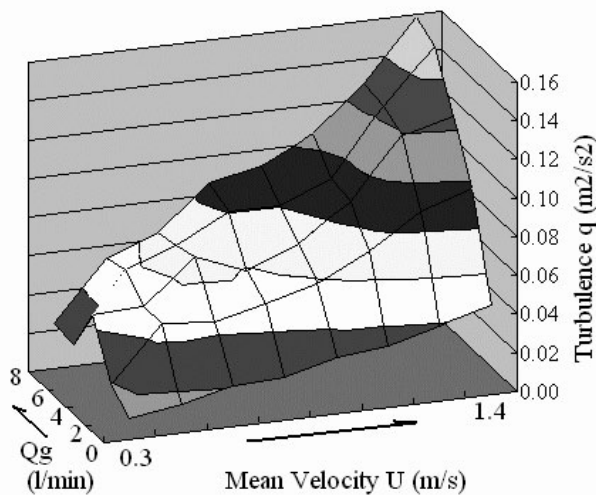


Figure 8: Turbulent intensity inside bubbly layer; $y/H < 0.16$

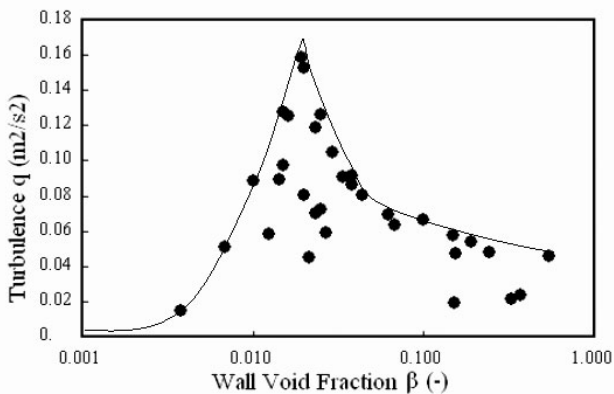


Figure 9: Turbulent intensity versus wall void fraction

Fig.8 shows the same data drawn as function of two flow rates. While the turbulence simply increases

with both flow rates, a new trend is found when it is plotted as a function of wall-void fraction β , as shown in Fig.9. Here β is defined by the local average void fraction inside the bubbly layer; $y/H < 0.16$, which is equivalent to the bubble-occupying area ratio on the wall. The plots say that the turbulence takes the highest value around $\beta = 0.02$, and decreases when larger area is provided.

4 SUMMARY

UVP has been applied to the measurement of turbulent bubbly channel flows to assess the modification of flow through bubbles. Summarizing the obtained data, the following scenario is deduced on the drag reduction by large bubbles. 1) Bubble-occupation on the wall reduces the total skin friction, and this provides the acceleration of liquid in the vicinity of the wall. 2) Turbulence inside the boundary layer increases with the acceleration. This effect propagates downward to alter the original flow within a certain spatio/temporal scale. 3) With these balance, the turbulence inside the boundary layer gets maximum at around 2% in area-based void fraction on the wall.

REFERENCES

- [1] Gabillet C, Colin C, Fabre J: Experimental Study of Bubble Injection in a Turbulent Boundary Layer, *Int. J. Multiphase Flow.* 28 (2002) 553-578.
- [2] Kitagawa A, Hishida K, Kodama Y: Flow Structure of Microbubble-laden Turbulent Channel Flow Measured by PIV Combined with the Shadow Image Technique, *Exp. Fluids.* 38 (2005), 466-475.
- [3] Murai Y, Oishi Y, Takeda Y, Yamamoto F: Turbulent Shear Stress Profiles in a Bubbly Channel Flow Assessed by Particle Tracking Velocimetry, *Exp. Fluids.* *In press* (2006) DOI 10.1007/s00348-006-0142-9
- [4] Suzuki Y, Nakagawa M, Aritomi M, Murakawa H, Kikura H, Mori M: Microstructure of the Flow Field Around a Bubble in Counter-Current Bubbly Flow, *Exp. Thermal Fluids Sci.* 26 (2002) 221-227.
- [5] Eckert S, Gerbeth G, Melnikov VI: Velocity Measurements at High Temperatures by Ultrasound Doppler Velocimetry Using an Acoustic Wave Guide, *Exp. Fluids.* 35 (2005), 381-388.
- [6] Murakawa H, Kikura H, Aritomi M: Application of Ultrasonic Doppler Method for Bubbly Flow Measurement Using Two Ultrasonic Frequencies. *Exp. Thermal Fluids Sci.* 29 (2005) 843-850.
- [7] Minagawa H, Fukuzawa T, Nakazawa Y, Yamada S, Shiomi Y: Measurements of Averaged Liquid Velocity Field Around Large Bubbles Using UVP, *Trans. Japan Soc. Mech. Eng.* 72 (2006) 345-352 (in Japanese).
- [8] Taishi T, Kikura H, Aritomi M: Effect of the Measurement Volume in Turbulent Pipe Flow Measurement by the Ultrasonic Velocity Profile Method – Mean Velocity Profile and Reynolds Shear Stress Measurement, *Exp. Fluids.* 32 (2002) 188-196.